Front. Optoelectron. 2014, 7(1): 84–90
DOI 10.1007/s12200-014-0361-2

RESEARCH ARTICLE

InAs/GaAs far infrared quantum ring inter-subband photodetector

Mohammad KARIMI[1], Kambiz ABEDI (✉)[2], Mahdi ZAVVARI[3]

1 Department of Electrical Engineering, Mahabad Branch, Islamic Azad University, Mahabad, Iran
2 Department of Electrical Engineering, Faculty of Electrical and Computer Engineering, Shahid Beheshti University, Tehran 1983963113, Iran
3 Department of Electrical Engineering, Urmia Branch, Islamic Azad University, Urmia, Iran

Abstract In this paper, we presented a numerical analysis of absorption coefficient, dark current and specific detectivity for InAs/GaAs quantum ring inter-subband photodetector (QRIP). 3D Schrödinger equation was solved using finite difference method and based on effective mass approximation. Dimensions of quantum ring (QR) were considered that inter-subband transition was to be accomplished for radiations of 20 μm. Resonant tunneling (RT) barriers were designed with tunneling probability of unity for electrons with energy of 0.062 meV to lower dark current of conventional QRIP. Numerical analyses show that inclusion of RT barriers can reduce dark current for about two orders of magnitude. Furthermore, specific detectivities for conventional QRIP and RT-QRIP were calculated respectively, and results at different temperatures were compared. It is suggested that specific detectivity for RT-QRIP is one order of magnitude higher than that for conventional QRIP. It is suggested that RT barriers considerably improve the specific detectivity of conventional QRIP at different temperatures.

Keywords quantum ring inter-subband photodetector (QRIP), dark current, spacefic detectivity, resonant tunneling (RT)

1 Introduction

Detection of infrared (IR) and terahertz (THZ) frequencies has attracted many interests because of its wide applications in the areas of night vision, thermal imaging, chemical analysis, nondestructive detection and remote sensing [1]. Recently, a new structure called quantum ring (QR) has been proposed to be used in the active region of semiconductor photodetectors, and quantum ring inter-subband photodetector (QRIP) can be designed to detect a wide range of electromagnetic frequencies from IR to THZ [2,3]. Detection of THz frequencies with cutoff wavelength at 175 μm using In(Ga)As QR photodetector has been reported by Lee et al. [4]. Bhowmick et al. have also reported high performance QR detector for 1–3 terahertz range with peak responsivity of 25 A/W, specific detectivity of 1×10^{16} $(\mathrm{cm} \cdot \mathrm{Hz}^{1/2})/\mathrm{W}$ and a total quantum efficiency of 19% [5]. However, because of more confinement in QR, the energy levels are closer to conduction band edge and hence it is expected to have higher dark current for a QRIP compared to other types of low dimensional semiconductor photodetectors. Dark current is an important factor which can affect the performance of any detector, and it must be as small as possible to attain high operation temperature and enhance specific detectivity. Huang et al. applied resonant tunneling (RT) barriers to suppress dark current of QRIP and enhance operation temperature and specific detectivity [6]. In this paper, first the electronic energy states and wave functions were obtained by numerical solution of 3D Schrödinger equation using finite difference method. Based on inter-subband transition, absorption coefficient was calculated and then dark current characteristics of a conventional InAs/GaAs QRIP were studied. Also, we showed reduction of dark current by inclusion of RT barriers and then specific detectivity for RT-QRIP was calculated and results were compared with conventional QRIP.

The paper is organized as follows: numerical analysis and simulation results are given and discussed in Section 2, the paper is concluded in Section 3.

Received July 8, 2013; accepted November 20, 2013

E-mail: k_abedi@sbu.ac.ir

2 Numerical analysis and simulation results

2.1 Eigenstates and eigenvalues within QR

To evaluate performance characteristics of a QRIP, it is needed to obtain eigenstates and eigenvalues within QR. For this purpose, we solve 3D Schrödinger equation for QR based on effective mass approximation and using finite difference method. 3D Schrödinger equation is equal to

$$-\frac{\hbar^2}{2m^*}\left(\frac{\partial^2}{\partial x^2}+\frac{\partial^2}{\partial y^2}+\frac{\partial^2}{\partial z^2}\right)\psi(x,y,z) + V(x,y,z)\psi(x,y,z) = E\psi(x,y,z), \quad (1)$$

where m^* is electron effective mass, and $V(x,y,z)$ is 3D confined potential energy as follows [7]:

$$V_e(x,y,z) = \begin{cases} 0, \left(\frac{R_1}{2}\right)^2 \leqslant x^2+y^2 \leqslant \left(\frac{R_2}{2}\right)^2, |z| \leqslant l, \\ E_c, \text{ other,} \end{cases} \quad (2)$$

$$m_e^*(x,y,z) = \begin{cases} m_i^*, \left(\frac{R_1}{2}\right)^2 \leqslant x^2+y^2 \leqslant \left(\frac{R_2}{2}\right)^2, |z| \leqslant l, \\ m_o^*, \text{ other,} \end{cases} \quad (3)$$

where E_c is the energy of conduction band edge between ring and barrier materials, m_i and m_o are electron mass in InAs ring and GaAs barrier, respectively, R_1, R_2 and z are inner and outer radius and height of QR, respectively. We numerically solve the equation for InAs/GaAs structure to obtain the electronic energy levels and wave functions within the ring.

The conduction band edge energy of GaAs barrier is changed from 0.77 to 0.513 eV due to high level of strain in this structure. Also, because of non-parabolic energy bands which are originated from higher orders of strain within ring, the effective mass is energy dependent. Position and energy dependent effective mass resulted from higher strain can be calculated using the following equation [8]:

$$\frac{1}{m_e(r,E)} = \frac{p^2}{\hbar^2} \times \left[\frac{2}{E+E_g(r)-V_e(r)} - \frac{1}{E+E_g(r)-V_e(r)+\Delta(r)}\right], \quad (4)$$

where p is momentum, E is electron energy, E_g is bandgap energy, and Δ is split-off energy. Using this equation, the effective mass of electron can be calculated by an iterative process.

In our calculations, we have considered QRs with dimensions of 10, 25 and 2 nm as inner and outer radius and height of ring, respectively. The obtained wave functions by solving 3D Schrödinger equation for ground state and first excited stated are shown in Figs. 1(a) and 1 (b), respectively.

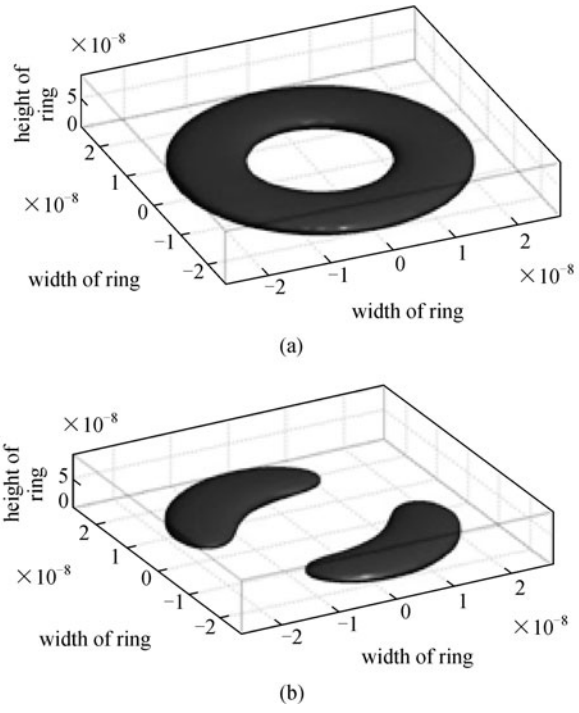

Fig. 1 (a) Isosurface of ground eigenstate of InAs/GaAs QR; (b) isosurface of first excited eigenstate of InAs/GaAs QR

2.2 Inter-subband absorption coefficient

To calculate the inter-subband absorption coefficient for our QRIP, we use the following relation [9]:

$$a(\hbar\omega) = \frac{\pi q^2}{\varepsilon_0 n_0 c m_0^2 V_{ac}} \frac{1}{\hbar\omega} \sum \left|\boldsymbol{a}.P_{fi}\right|^2 N(\hbar\omega), \quad (5)$$

where q is electron charge, c is speed of light, V_{ac} is effective volume of a QR layer, $\boldsymbol{a}$ is incidence light polarization vector, P_{fi} is momentum matrix element and $N(\hbar\omega)$ is density of states which can be calculated from [10]:

$$N(\hbar\omega) = \int_{-\infty}^{\infty} \frac{\hbar\gamma_{fi}/\pi}{(E-E')^2+(\hbar\gamma_{fi})^2} \times \frac{1}{\sqrt{2\pi}\sigma} \exp\left(-\frac{(E_{fi}-E')^2}{(\sqrt{2}\sigma\gamma_{fi})^2}\right) \times \left(f_i(E')-f_f(E')\right) dE', \quad (6)$$

where E_{fi} is transition energy between subbands of f and i. The first term in Eq. (6) corresponds to Lorentzian function with line-width of $\hbar\gamma_{fi}$, which appears due to different phonon scattering mechanism and thermal broadening of energy states. Also, due to self-assembled growth technique, all QRs do not have identical dimensions and hence energy levels would not be same for all rings. Such non-uniformity leads to a broadening in energy levels and is modeled as inhomogeneous broadening (IHB) which appears as a Gaussian function in equation with line-width of σ. Using Eq. (5), we calculate the inter-subband absorption coefficient and results are shown in Fig. 2 for different homogeneous broadening (HB) energies. According to Fig. 2, absorption peak decreases as HB increases from 2 to 10 meV. However, when IHB is 40 meV, the reduction effect of HB can be neglected. Because of large dipole momentum between ground state and first excited state, we consider the transition between these levels and neglect transitions between other energy states. As can be seen, absorption coefficient is around $4.3 \times 10^4\ \mathrm{cm}^{-1}$ at wavelength of 20 μm for HB of 5 meV and IHB of 15 meV.

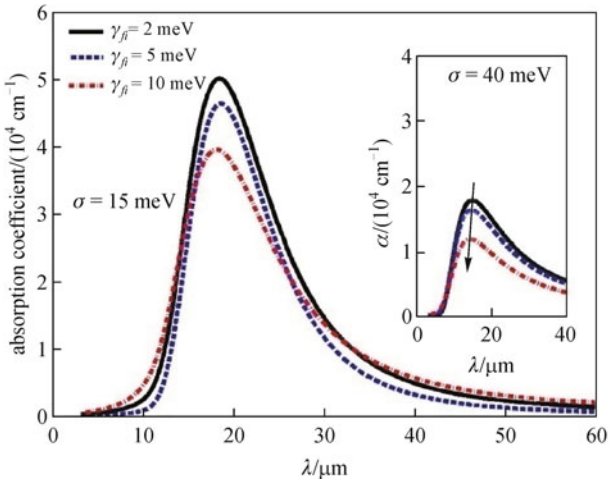

Fig. 2 Absorption coefficient of QRIP as function of wavelength for different values of homogeneous broadening (inset figure shows absorption coefficient of QRIP versus wavelength for different values of HB when inhomogeneous broadening is 40 meV)

In order to investigate the influence of QR dimension on photodetector performance, absorption spectrum of QRs is calculated as a function of wavelength for different values of outer radius and results are shown in Fig. 3. As can be seen, absorption spectrum experiences a redshift from 20 to 45 μm when outer radius increases from 25 to 40 nm. Changing the QRs dimension leads to decreasing the space between energy levels within QRs, and hence radiations with higher wavelength can be absorbed. This fact can be used for designing wavelength tunable QRIP through changing QRs dimension.

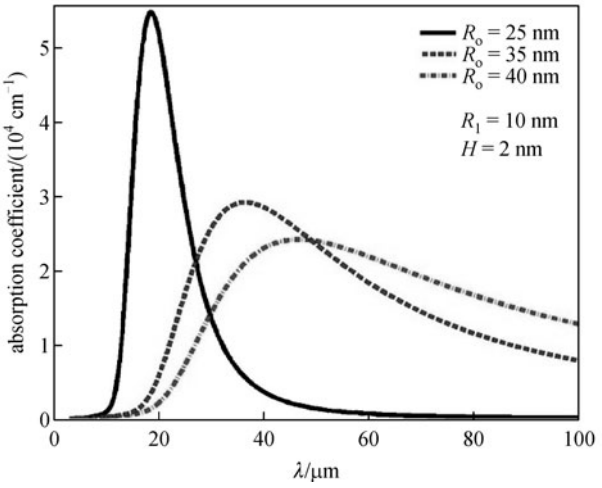

Fig. 3 Absorption coefficient of QRIP as function of wavelength for different values of outer radius with R_1 = 10 nm and H = 2 nm

2.3 Dark current

Dark current for QR detector is originated from thermally excited electrons when there is no incident light, and it can be written as [11]

$$I_{\mathrm{D}}(V) = qn(V)\nu(V)A, \tag{7}$$

where $\nu(V)$ is the average electron drift velocity in the barrier material, A is the detector area and $n(V)$ is density of thermally electrons which can be calculated from [11]

$$n(V) = \int N(E)f(E)T(E,V)\mathrm{d}E, \tag{8}$$

where $f(E)$ is Fermi-Dirac distribution function, $T(E,V)$ is the transmission probability through device and $N(E)$ is the density of states expressed by [11]

$$N(E) = \sum_i \frac{2N_{\mathrm{D}}}{L_{\mathrm{p}}}\frac{1}{\sqrt{2\pi}\sigma}\exp\left(-\frac{(E-E_i)^2}{2\sigma^2}\right) + \frac{4\pi m^*}{L_{\mathrm{p}}\hbar^2}H(E-E_{\mathrm{W}}) + \frac{8\pi\sqrt{2}}{\hbar^3}m^{*3/2}\sqrt{E-E_{\mathrm{c}}}H(E-E_{\mathrm{c}}), \tag{9}$$

where N_{D} is the density of quantum dot surface, L_{p} is the absorption length, E_i is the energy levels within QR and $H(E)$ is the step function. The first term in Eq. (9) corresponds to density state of QR, the second term expresses the wetting layer density of states which E_{w} is wetting layer energy, and the last term describes barrier bulk density of states with conduction bandage energy of E_{C}.

Figure 4 shows the calculated dark current as a function

of applied bias for different temperatures. According to figure, dark current increases with applied bias which means that dark electrons move with higher drift velocity. On the other hand, for higher temperatures, dark current reaches to higher levels which describe thermally nature of generated dark carriers. Such an increase in dark current results in reduction of overall performance and hence the operation temperature of QRIP is limited. Results show that the dark current for 80, 120 and 160 K at 0.4 V is in the order of 10^{-6}, 10^{-3} and 10^{-1} A/cm^2, respectively. According to results incorporation expensive and large cryogenic cooling systems for improvement the operation temperature is mandatory. To attain higher specific detectivity at higher operation temperature, a QRIP with low dark current is desired. Low dark current QRIP can be realized using RT barriers which blocks thermally excited electrons. This structure consists of two AlGaAs barriers and one InGaAs well which provide an identical pass with transmission coefficient near unity. Only the photons with energies of inter-subband transition between QR states and this tunneling state can be absorbed and make photocurrent. Figure 5 shows the heterostructure schematic of RT-QRIP and one period of its conduction band profile with RT barriers. We calculate tunneling probability for the structure and result is shown in Fig. 6. According to figure, tunneling probability is unity for electrons with energy of 0.062 eV which corresponds to inter-subband transition energy of 20 μm and reduces rapidly when the electrons energy moves away from resonance energy. Figure 7 shows calculated dark current for RT-QRIP. Results show that the dark current is in the order of 10^{-2}, 10^{-4} and 10^{-8} A/cm^2 for temperatures of 160, 120 and 80 K at 0.4 V, respectively. It is evident that dark current of RT-QRIP reduces compared to the dark current of conventional QRIP. For better comparison, dark current of conventional QRIP and RT-QRIP are sketched in Fig. 8 as a function of temperature and for bias voltage of 0.4 V. According to figure, although the dark current increases with temperature, however RT barriers considerably lower the dark current compared to conventional QRIP.

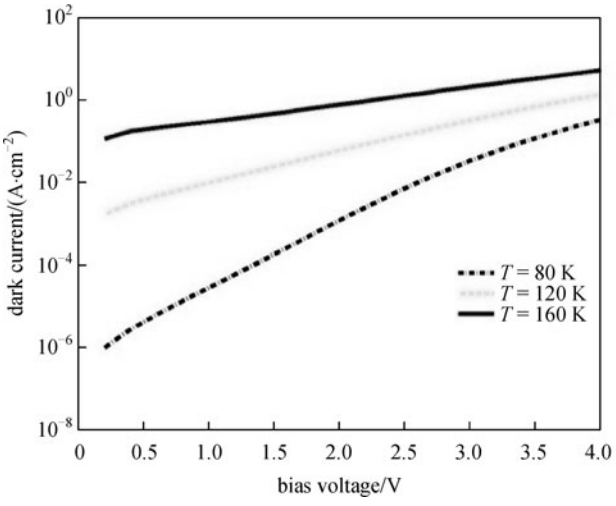

Fig. 4 Dark current of QRIP versus bias voltage for different temperatures

2.4 Specific detectives

Specific detectivity (D^*), is a main characteristic figure of merit used to rate detector performance and equal to inverse of noise equivalent power (NEP) and can be calculated from [12–15]

$$D^* = R\frac{\sqrt{A\Delta f}}{i_n}, \tag{10}$$

where Δf is the bandwidth, R is responsivity and i_n is the noise current of the device and is equal to

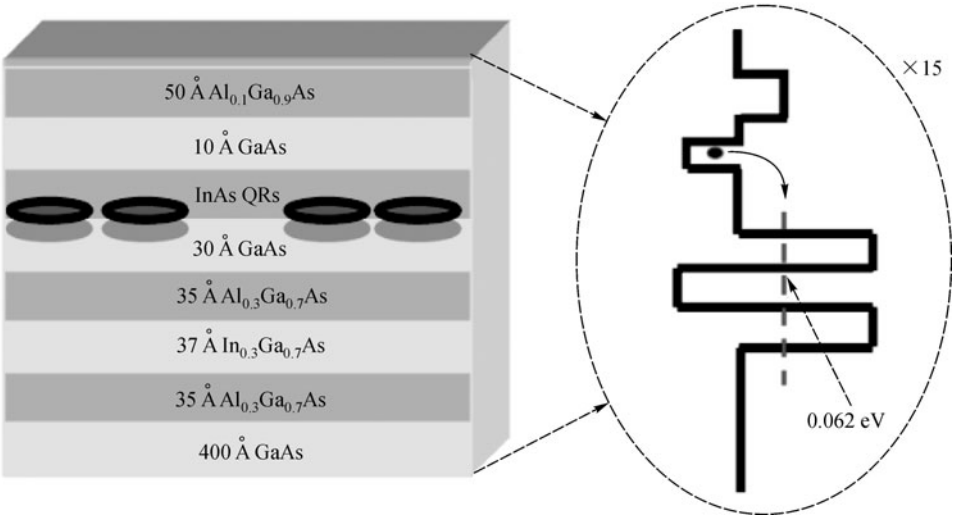

Fig. 5 Schematic of RT-QRIP, and the inset depicts one stack of QR layers with RT barriers

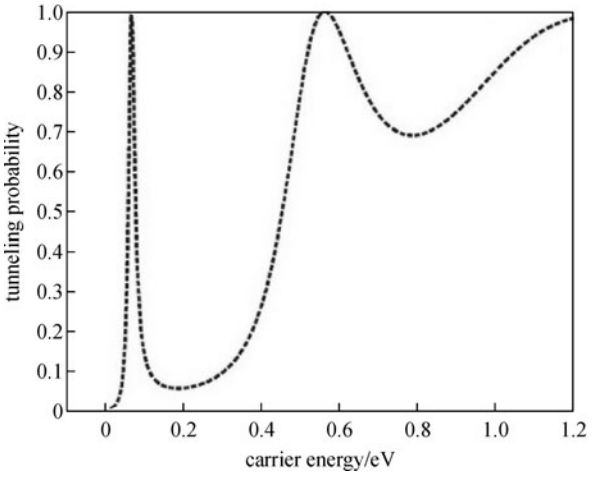

Fig. 6 Calculated tunneling probability for RT structure

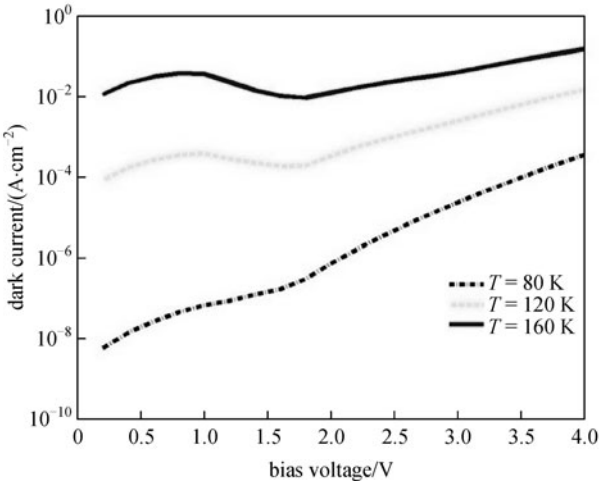

Fig. 7 Dark currents of RT-QRIP at different temperatures

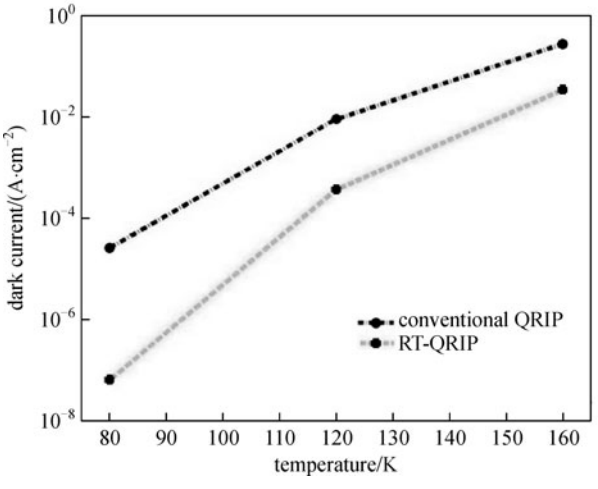

Fig. 8 Dark currents of conventional QRIP and RT-QRIP versus temperature at 1 V

$i_n = \sqrt{4qI_D g_n \Delta f}$, where g_n is noise gain.

Lower value of dark current leads to higher level of specific detectivity and hence one can expect an enhanced specific detectivity for RT-QRIP due to its low dark current.

Figure 9 illustrates the calculated specific detectivity for conventional InAs/GaAs QRIP versus bias voltages for different temperatures. For higher bias voltage, the specific detectivity decreases due to the increase in dark current. Also, as can be seen from the figure, for higher temperatures, the specific detectivity of conventional QRIP is reduced due to strong dependence of dark current on temperature. According to Fig. 9, D^* is in the order of ~10^6, ~10^7 and ~10^9 (cm·Hz$^{1/2}$)/W at 160, 120 and 80 K, respectively.

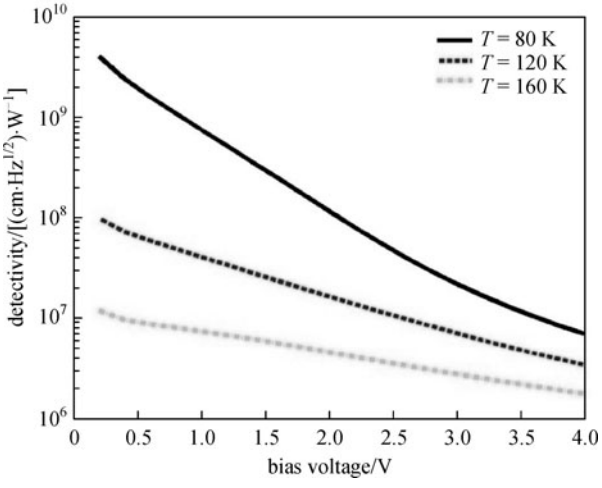

Fig. 9 Specific detectivity of conventional QRIP versus bias voltage for different temperatures

To investigate the influence of inclusion RT barriers, we calculate the specific detectivity for RT-QRIP and the results are shown in Fig. 10. According to the figure, D^* is in the order of ~10^7, ~10^8 and ~10^{10} (cm·Hz$^{1/2}$)/W at 160, 120 and 80 K, respectively. It is evident that specific detectivity is increased in comparison to conventional QRIP. However, the degradation of this parameter with bias and temperature still remains.

Temperature is a critical parameter, which can affect the performance of a photodetector. High operation temperature photodetectors are desired to avoid incorporation of large and high cost cryogenic cooling systems. Figure 11 shows the dependence of conventional QRIP and RT-QRIP specific detectivity on temperature at applied bias of 1 V. As we expect, D^* is higher for RT-QRIP than conventional QRIP due to lower dark currents. According to Fig. 11, using RT barriers leads to enhancement of specific detectivity about two orders of magnitude for temperature of 80 K and about one order of magnitude for temperature of 160 K.

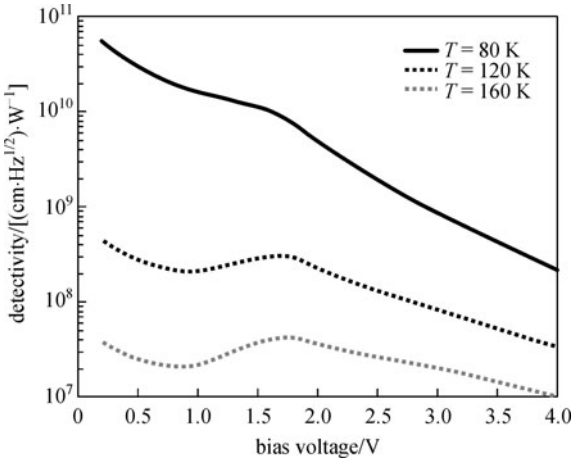

Fig. 10 Specific detectivity of RT-QRIP versus bias voltages for different temperatures

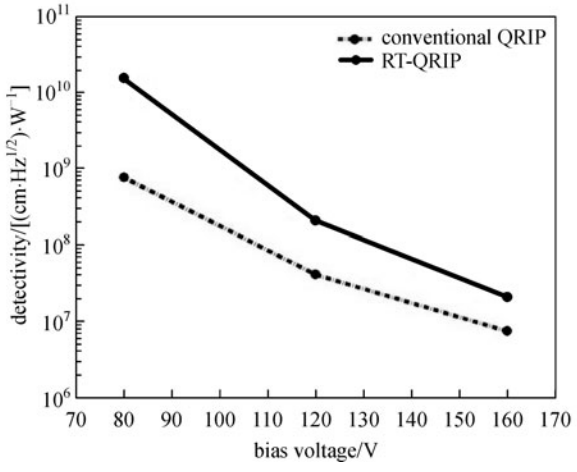

Fig. 11 Specific detectivity of conventional QRIP and RT-QRIP as function of temperature

3 Conclusions

Numerical analysis of absorption coefficient, dark current and specific detectivity of QRIP was presented. By solving 3D Schrödinger equation, wave functions and energy levels within ring were calculated. It was shown that QRIP has absorption coefficient peak about 4.3×10^4 cm^{-1} at 20 μm wavelength. Dark current and specific detectivity of QRIP with and without using RT barrier was studied. According to results, inclusion of RT barriers reduces dark current of QRIP for about two orders of magnitude. It is suggested that RT barriers considerably improve the specific detectivity of conventional QRIP at different temperatures.

References

1. Hsu B C, Lin C H, Kuo P S, Chang S, Chen P, Liu C, Lu J H, Kuan C H. Novel MIS Ge-Si quantum-dot infrared photodetectors. Electron Device Letters, IEEE, 2004, 25(8): 544–546
2. Dai J H, Lee J H, Lin Y L, Lee S C. In(Ga)As quantum rings for terahertz detectors. Japanese Journal of Applied Physics, 2008, 47 (4): 2924–2926
3. Ling H S, Wang S Y, Lee C P, Lo M C. Characteristics of In(Ga)As quantum ring infrared photodetectors. Journal of Applied Physics, 2009, 105(3): 034504-1–034504-4
4. Lee J H, Dai J H, Chan C F, Lee S C. In(Ga)As quantum ring terahertz photodetector with cutoff wavelength at 175 μm. Photonics Technology Letters, IEEE, 2009, 21(11): 721–723
5. Bhowmick S, Huang G, Guo W, Lee C S, Bhattacharya P, Ariyawansa G, Perera A G U. High-performance quantum ring detector for the 1–3 terahertz range. Applied Physics Letters, 2010, 96(23): 231103-1–231103-3
6. Huang G, Guo W, Bhattacharya P, Ariyawansa G, Perera A G U. A quantum ring terahertz detector with resonant tunnel barriers. Applied Physics Letters, 2009, 94(10): 101115-1–1101115-3
7. Li S S, Xia J B. Electronic states of InAs/GaAs quantum ring. Journal of Applied Physics, 2001, 89(6): 3434–3437
8. Chen J H, Liu J L. A numerical method for exact diagonalization of semiconductor quantum dot model. Computer Physics Communications, 2010, 181(5): 937–946
9. Kochman B, Stiff-Roberts A D, Chakrabarti S, Phillips J D, Krishna S, Singh J, Bhattacharya P. Absorption, carrier lifetime, and gain in InAs-GaAs quantum-dot infrared photodetectors. IEEE Journal of Quantum Electronics, 2003, 39(3): 459–467
10. Mir A, Ahmadi V. Design and analysis of a new structure of InAs/GaAs QDIP for 8–12 μm infrared windows with low dark current. Journal of Modern Optics, 2009, 56(15): 1704–1712
11. Su X H, Chakrabarti S, Bhattacharya P, Ariyawansa G, Perera A G U. A resonant tunneling quantum-dot infrared photodetector. IEEE Journal of Quantum Electronics, 2005, 41(7): 974–979
12. Towe E, Pan D. Semiconductor quantum-dot nanostructures: their application in a new class of infrared photodetectors. IEEE Journal of Selected Topics in Quantum Electronics, 2000, 6(3): 408–421
13. Zavvari M, Ahmadi V, Mir A, Darabi E. Quantum dot infrared photodetector enhanced by avalanche multiplication. Electronics Letters, 2012, 48(10): 589–591
14. Zavvari M, Ahmadi V. Dynamics of avalanche quantum dot infrared photodetectors. Modern Physics Letters B, 2012, 26(32): 1250216-1–1250216-10
15. Zavvari M, Ahmadi V. Quantum-dot-based id-IR single-photon detector with self-quenching and self-recovering operation. Electron Device Letters, IEEE, 2013, 34(6): 783–785

Mohammad Karimi was born in Naghadeh, Iran, in 1988. He received the M.S. degree in electrical engineering from Islamic Azad University, Ahar, Iran, in 2013. His M.Sc thesis focused on the "Design and Analysis of InAs/GaAs Quantum Ring Photodetector for Long Wavelength Applications". His research interests include low dimensional quantum structures, with specialization in the field of QDIPs, QRIPs and lasers.

Kambiz Abedi was born in Ahar, Iran, in 1970. He received his B.S. degree from University of Tehran, Iran, in 1992, his M.S. degree from Iran University of Science and Technology, Tehran, Iran, in 1995, and his Ph.D. degree from Tarbiat Modares University, Tehran, Iran, in 2008, all in electrical engineering. His research interests include design, circuit modeling and numerical simulation of optoelectronic devices, semiconductor lasers, optical modulators, optical amplifiers and detectors. Dr. Abedi is currently an Assistant Professor at Shahid Beheshti University, Tehran, Iran.

Mahdi Zavvari was born in Salmas, Iran, in 1981. He received the B.S. degree from Tabriz University in 2004, M.S. and Ph.D. degrees from Islamic Azad University science and research branch in 2007 and 2012, respectively, all in electronic engineering. He is currently academic staff of Urmia branch, Islamic Azad University and his research interest is on quantum dot/ring photodetectors, single photon detectors, avalanche photodiodes and lasers.